Molecular Biology of the Cell
Vol. 6, 851–869, July 1995

The Metalloproteinase Matrilysin Is Preferentially Expressed by Epithelial Cells in a Tissue-restricted Pattern in the Mouse

Carole L. Wilson, Kathleen J. Heppner, Laura A. Rudolph, and Lynn M. Matrisian*

Department of Cell Biology, Vanderbilt University Medical School, Nashville, Tennessee 37232

Submitted July 25, 1994; Accepted May 1, 1995
Monitoring Editor: Keith R. Yamamoto

To explore the role of the matrix metalloproteinase matrilysin (MAT) in normal tissue remodeling, we cloned the murine homologue of MAT from postpartum uterus using RACE polymerase chain reaction and examined its pattern of expression in embryonic, neonatal, and adult mice. The murine coding sequence and the corresponding predicted protein sequence were found to be 75% and 70% identical to the human sequences, respectively, and organization of the six exons comprising the gene is similar to the human gene. Northern analysis and in situ hybridization revealed that MAT is expressed in the normal cycling, pregnant, and postpartum uterus, with levels of expression highest in the involuting uterus at early time points (6 h to 1.5 days postpartum). The mRNA was confined to epithelial cells lining the lumen and some glandular structures. High constitutive levels of MAT transcripts were also detected in the small intestine, where expression was localized to the epithelial Paneth cells at the base of the crypts. Similarly, MAT expression was found in epithelial cells of the efferent ducts, in the initial segment and cauda of the epididymis, and in an extra-hepatic branch of the bile duct. MAT transcripts were detectable only by reverse transcription-polymerase chain reaction in the colon, kidney, lung, skeletal muscle, skin, stomach, juvenile uterus, and normal, lactating, and involuting mammary gland, as was expression primarily late in embryogenesis. Analysis of MAT expression during postnatal development indicated that although MAT is expressed in the juvenile small intestine and reproductive organs, the accumulation of significant levels of MAT mRNA appears to correlate with organ maturation. These results show that MAT expression is restricted to specific organs in the mouse, where the mRNA is produced exclusively by epithelial cells, and suggest that in addition to matrix degradation and remodeling, MAT may play an important role in the differentiated function of these organs.

INTRODUCTION

Matrix metalloproteinases (MMPs) comprise a family of enzymes that are capable of degrading the major components of the extracellular matrix (ECM) under physiological conditions (reviewed in Alexander and Werb, 1989; Matrisian, 1990, 1992; Woessner, 1991). Changes in the ECM can have a profound effect on a wide variety of cellular responses, from adhesion and proliferation to cell migration and differentiation. MMPs have been implicated in several normal processes of tissue remodeling, such as embryonic development, wound healing, trophoblast implantation, and organ morphogenesis, as well as various disease states, including tumor invasion and metastasis, rheumatoid arthritis, and osteoporosis. The MMPs are grouped loosely by substrate specificity and include the collagenases, the 72- and 92-kDa gelatinases, and the stromelysins, which include the stromelysin-like

* Corresponding author: Department of Cell Biology, Vanderbilt University Medical Center, Nashville, TN 37232-2175.

enzyme matrilysin (MAT). In general, the stromelysin class of MMPs can degrade a broad range of substrates, such as fibronectin, laminin, elastin, denatured collagen and collagen fragments, and proteoglycans (reviewed in Birkedal-Hansen *et al.*, 1993). MAT is structurally distinct from the other known MMPs in that it consists of only the three domains essential for activity: the signal or presequence to direct secretion of the zymogen from the cell, the prosequence to maintain latency, and the Zn^{2+}-binding catalytic domain. The other MMPs contain at least one additional domain that is not required for proteolytic activity but may influence substrate specificity. For example, the carboxy-terminal vitronectin-like domain in collagenase endows this enzyme with the ability to recognize and cleave fibrillar collagens (Murphy *et al.*, 1992; Hirose *et al.*, 1993).

Human MAT was originally cloned from a cDNA library prepared from a mixture of human tumors (Muller *et al.*, 1988), and recently was isolated from mesangial cells (Marti *et al.*, 1992). Characterization of the genomic structure showed that organization of the first five exons of the six that comprise the human gene is similar to other MMP family members (Gaire *et al.*, 1994). Furthermore, the MAT promoter contains conserved AP-1 and PEA3 elements, which in part mediate the up-regulation of MAT transcripts in response to epidermal growth factor and phorbol esters (Gaire *et al.*, 1994). MAT was originally termed pump-1 (putative metalloproteinase) based on its homology to stromelysin-1 and the collagenases; recombinant pump-1 protein expressed in COS cells (Quantin *et al.*, 1989) was found to have identical properties to a small uterine MMP (ump) isolated from the rat (Sellers and Woessner, 1980). In the rat uterus, MAT activity peaks on the day after parturition, suggesting that the enzyme is involved in involution, or resorption, of the uterus (Woessner and Taplin, 1988; Quantin *et al.*, 1989).

Although expression of MAT has been associated primarily with neoplastic lesions (Basset *et al.*, 1990; McDonnell *et al.*, 1991; Pajouh *et al.*, 1991; Newell *et al.*, 1994), evidence for its expression in normal human tissues is beginning to accumulate. For example, in the menstrual cycle, MAT mRNA and protein localize to the glandular epithelium of the endometrium during the proliferative, late secretory, and menstrual phases (Rodgers *et al.*, 1993). Recently, the protein has been found in the outer root sheath of the hair follicles and in the eccrine glands of adult skin (Karelina *et al.*, 1994). In these examples, MAT is restricted to the epithelial component, whereas the majority of other MMPs are produced primarily by mesenchymal cells in the stroma (reviewed in Crawford and Matrisian, 1995). The ability of MAT to digest basement membrane components laminin, type IV collagen, and entactin in vitro (Miyazaki *et al.*, 1991; Murphy *et al.*, 1991; Sires *et al.*, 1993) points to a role for this enzyme in basement membrane degradation.

The unique structure of the MAT protein and its pattern of localization to epithelial tissues in some normal and pathological conditions suggest that this MMP may function in tissue reorganization in vivo in a manner distinct from that of other MMPs. An understanding of the role of MAT in normal tissue remodeling could provide insight into the role of this enzyme in tumor progression. The mouse is an ideal model system in which to explore the functions of MAT in vivo, particularly because this organism can be genetically manipulated. Therefore, we cloned the cDNA and gene for murine MAT to compare with the human sequence, and examined its expression in normal tissues in the mouse.

MATERIALS AND METHODS

Tissue Preparation and RNA Extraction

Uterine and mammary tissue, as well as embryos at different stages of development, were obtained from outbred ICR mice. Other tissues were dissected from C57BL/6N mice or B6/DBA F_1 hybrids. Mice at 8 wk of age were considered to be adult, and the day on which pups were found was designated the P1 stage. In females, stages of the estrus cycle were determined by histological analysis of vaginal smears as described by Rugh (1968). Animals were killed by cervical dislocation under inhalation anesthesia, and dissected tissue to be used for RNA extraction was quickly frozen on dry ice or in liquid nitrogen. Tissue was homogenized in a guanidinium thiocyanate-acid phenol solution, and total RNA was extracted essentially as described by Chomczynski and Sacchi (1987). Tissues to be used for in situ hybridization were immediately fixed in either formalin or fresh 4% paraformaldehyde in phosphate-buffered saline (PBS). Tissues were then dehydrated and processed for embedding in paraffin by standard procedures. Specific regions of the small and large intestines were identified according to the anatomical guide to laboratory animals published by Popesko *et al.* (1992). Tissue was dissected from approximately the middle of each region as mapped in the guide.

cDNA Cloning

The 3′ end of the cDNA for murine MAT was cloned using the 3′ rapid amplification of cDNA ends (RACE) technique as described by Frohman *et al.* (1988). Primers used for these studies were generated in the Vanderbilt University Medical Center Oligonucleotide Synthesizing Facility, unless otherwise noted. Other reagents for 3′ RACE were obtained from Perkin-Elmer (Norwalk, CT). Approximately 1 μg of total cellular RNA isolated from day 1 postpartum uterus was mixed with the following reagents in a final volume of 20 μl: 5 mM $MgCl_2$, 10 mM Tris-HCl, pH 8.3, 50 mM KCl, 500 μM each dNTP, 20 U RNase inhibitor, 50 U Moloney murine leukemia virus reverse transcriptase, and 0.5 μg of an adaptor-poly d(T) primer [5′-GACTCGAGTCGACGCGGCCGC$(T)_{17}$-3′]. The adaptor sequence contained *Xho*I, *Sal*I, and *Not*I restriction enzyme sites as part of the polymerase chain reaction (PCR) and cloning strategy. Reverse transcription (RT) was carried out at 45°C for 1 h, then repeated with additional reverse transcriptase. The reaction was diluted to 50 μl, and 1 μl was used for PCR amplification under the following conditions: 0.5–5.0 mM $MgCl_2$, 10 mM Tris-HCl, pH 8.3, 50 mM KCl, 200 μM each dNTP, and 25 pmol of each primer in 50 μl final volume. The forward primer was derived from the beginning of the exon 3 sequence (MMEX3; see below) and contained a *Hin*dIII site at the 5′ end (5′-GCAAGCTT-CTTACCTCGGATCG-

TAGTGGA-3′), whereas the reverse primer was specific for the adaptor sequence (5′-GACTCGAGTCGACGCGGCCGC-3′). The initial reaction consisted of a 40-min extension as described by Frohman *et al.* (1988). Forty cycles of PCR were then carried out (1 min at 95°C, 1 min at 55°C, and 3 min at 72°C), followed by extension at 72°C for 15 min. Twenty-five microliters of each sample was electrophoresed in a 1% agarose gel. Although products could not be visualized by ethidium bromide staining, two closely migrating bands of approximately 700 bp were detected by Southern blotting and hybridization with a radiolabeled MMEX3 fragment (see below) in the PCR reaction that contained 3 mM $MgCl_2$. The remainder of that PCR reaction was digested with *Hin*dIII and *Xho*I, ligated into an appropriately cut pGEM7Zf(+) vector, and used to transform competent DH5α bacteria. Colonies were screened by hybridization with MMEX3. Three positive clones were identified, one of which was shown to contain murine MAT sequence (MMAT2) by Southern blotting and dideoxy sequencing (Sequenase Version 2.0 DNA Sequencing kit, United States Biochemical, Cleveland, OH). The poly A tail was removed by cleavage at an *Apa*LI site following the polyadenylation sequence to yield the plasmid pGEM7-MMATAH. The cDNA fragment was excised from this plasmid with *Hin*dIII and *Apa*I for use as a hybridization probe. All ^{32}P-labeled probes were prepared using a random priming kit (Boehringer Mannheim, Indianapolis, IN). Restriction enzymes were purchased from either Promega (Madison, WI) or New England Biolabs (Beverly, MA).

The 5′ RACE System from Life Technologies (Gaithersburg, MD) was used for cloning the 5′ end of murine MAT cDNA, again from 1 μg of total RNA from day 1 postpartum uterus. RNA was mixed with 2 pmol of the reverse primer derived from the exon 6 sequence (5′-CCAGTGAGTGCAGACCGT-3′); RT, dCTP tailing, and DNA purification were performed as directed by the manufacturer. PCR amplification was carried out as described for 3′ RACE, except 2.5 mM $MgCl_2$ and 20 pmol of each primer were used. The forward, or anchor, primer (Life Technologies; 5′-CUACUACUACUAGGCCACGCGTCGACTAGTACGGGIIGGGIIGGGIIG-3′) contained three restriction enzyme sites, *Mlu*I, *Sal*I, and *Spe*I, and could anneal to the poly C tail on the cDNA by virtue of the stretch of G bases. The reverse primer contained a sequence spanning the boundary between exons 3 and 4 in MMAT2 as well as an *Xho*I restriction enzyme site (5′-GCCTCGAG-CTGTCTCCATGATCTCTCCT-3′). Forty cycles of amplification were performed using the same parameters as for 3′ RACE. One-half of the PCR reaction was purified using the WIZARD PCR Prep Purification System (Promega) and used for a second round of amplification (30 cycles). For this round, the Universal Amplification Primer in the 5′ RACE kit was used as the forward primer (5′-CUACUACUACUAGGCCACGCGTCGACTAGTAC-3′). A product of ~600 bp was detected by gel electrophoresis, Southern blotting, and hybridization with a radiolabeled fragment containing exon 2 from the murine gene (see below). The DNA was purified using a WIZARD-PCR column, cut with *Xho*I and *Mlu*I, and ligated into pGEM7Zf(+) linearized with the same enzymes. Colonies obtained after transformation were screened by hybridization using the exon 2 genomic fragment. By sequencing, three positive clones were obtained, one of which contained a sequence corresponding to exons 1, 2, and 3 (MMAT1); the other 2 clones were missing exon 1 sequence and were not analyzed further.

Isolation and Southern Blot Analysis of Genomic Clones

A λ2001 library prepared from strain C3H genomic DNA (obtained from C.V.E. Wright, Vanderbilt University) was screened at low stringency (35% formamide, 35°C hybridization, 37°C washes) using a radiolabeled human MAT cDNA fragment (Muller *et al.*, 1988). From the single positive clone obtained, a 500-bp *Acc*I fragment was subcloned into pGEM7Zf(+) and sequenced, and was shown to contain exon 3 based on homology to the human MAT sequence. A 200-bp *Nla*IV fragment from this subclone was ligated into a *Sma*I-cut pGEM7Zf(+) vector and the construct was called MMEX3. The clone contained all 149 bp of exon 3, and 15 bp and 11 bp of 5′ and 3′ flanking intron sequence, respectively.

The MMEX3 fragment was used to probe a λFIXII mouse genomic library prepared from strain 129/Sv DNA (Stratagene, La Jolla, CA) under high stringency conditions. Three identical clones were identified, one of which was used for DNA isolation. The insert of approximately 15 kb was excised with *Not*I and subcloned into pGEM5Zf(+). From this plasmid other subclones were generated for mapping and sequencing of the gene: pGEM7-MuPB1, containing a 6.5-kb *Bam*HI fragment (exons 2, 3, 4, 5, and 6); pGEM5-MuPNRV, containing a 6-kb *Not*I–*Eco*RV fragment (exons 1, 2, and most of 3); pGEM7-MMATGEX1, containing a 700-bp *Eco*RI–*Sph*I fragment (exon 1); and PGEM7-SRVHE, containing a 500-bp *Hin*dIII–*Eco*RI fragment (exon 2). Exons were mapped by restriction enzyme digestion and Southern blotting using mouse MAT cDNA fragments and a *Xho*I–*Bst*EII fragment from the human cDNA containing sequence corresponding to exons 1 and 2. Exon-intron boundaries were determined by sequencing and comparison to the murine cDNA and to the human gene.

Northern Blotting

Ten to 20 μg of total cellular RNA were electrophoretically separated in 1% agarose gels containing formaldehyde and morpholinopropanesulfonic acid buffer, and transferred to nitrocellulose. Blots were hybridized at 42°C under high-stringency conditions (50% formamide and 5× SSC) using the radiolabeled MAT cDNA fragment from pGEM7-MMATAH. Washes were carried out at 50°C in 0.1× SSC. After stripping the blot, hybridization with cDNA corresponding to the mouse cytoplasmic 7S RNA (Balmain *et al.*, 1982) was used to control for loading.

RT-PCR

MAT transcripts were amplified from approximately 0.25–0.5 μg of total RNA using the Thermostable rTth Reverse Transcriptase RNA PCR Kit (Perkin-Elmer) as described by the manufacturer. The forward primer was derived from cDNA sequence that spans exons 4 and 5 (5′-GTGAGGACGCAGGAGTGAAC-3′) and the reverse primer from the 3′-untranslated region in exon 6 (5′-ACAGGTGCAGCTCAGGAAGG-3′). An annealing temperature of 63°C was used both for the RT reaction and for 35 cycles of PCR, giving rise to a product of 292 bp. For most tissue RNAs, mouse glyceraldehyde phosphate dehydrogenase was amplified in a separate reaction to verify the presence of intact mRNA. The forward and reverse primers used were 5′-TGAAGGTCGGTGTGAACGGATTTGGC-3′ and5′-CATGTAGGCCATGAGGTCCACCAC-3′,respectively,yielding a product of 983 bp. For embryonic RNAs, amplification of murine 72-kDa gelatinase mRNA was used as the control (forward primer, 5′-GGTGGCAATGCTGATGGACA-3′; reverse primer, 5′-TTGGTTCTCCAGCTTCAGGT-3′).

Riboprobe Preparation and In Situ Hybridization

Plasmid pGEM7-MMATAH (containing MMAT2 sequence but lacking the poly A tail) was linearized with *Apa*I to generate the antisense MAT riboprobe using T7 RNA polymerase. The *Hin*dIII–*Apa*I fragment from pGEM7-MMATAH was subcloned into the Bluescript KS vector to use the same polymerase to prepare the sense-strand riboprobe from *Hin*dIII-linearized template. Plasmid D4CL9B containing 421 bp of the cDNA for cryptdin-1 in Bluescript SK(−) was generously provided by A. Ouellette (Harvard Medical School, Boston, MA). To generate templates for transcription using either T3 (antisense) or T7 (sense) RNA polymerase, the plasmid was linearized with *Hin*dIII or *Bam*HI, respectively. In vitro transcription was performed using [^{35}S]UTP (Amersham, Arlington Heights, IL).

Sections of each tissue from 5–7 μm were treated as described previously (McDonnell *et al.*, 1991), except that prehybridization of the slides, as well as hybridization, was carried out at 50°C. For autoradiography, slides were dipped in photographic emulsion (type NTB2; Kodak, Rochester, NY) and exposed for 5 days to 3 wk. After exposure, the slides were developed and the sections counterstained with either 0.2% toluidine blue or Mayer's hematoxylin.

BrdU Immunohistochemistry

Mice were injected intraperitoneally with 5-bromo-2-deoxyuridine (BrdU; Sigma) in 10 mM PBS at 50 mg/kg body weight. After 1 h, animals were killed and the small intestine was removed and fixed in 4% paraformaldehyde. Tissue was embedded in paraffin and sectioned. Staining for BrdU was performed essentially as described previously (Ward *et al.*, 1988). Briefly, sections were incubated with a 1:400 dilution of a monoclonal rat antibody against BrdU (Accurate Chem. and Sci., Westbury, NY) in PBS, followed by a 1:100 dilution of biotinylated rabbit anti-rat antibody (Vector Laboratories, Burlingame, CA) in PBS. Labeled cells were visualized using an avidin-biotin peroxidase complex (Vectastain ABC kit, Vector Laboratories) and AEC chromogen (Biomeda, Foster City, CA). Sections were counterstained with Mayer's hematoxylin.

RESULTS

Cloning of the Mouse MAT cDNA and Gene

The murine homologue of MAT was cloned from postpartum uterus using the RACE technique (Frohman *et al.*, 1988) to amplify the 5′ and 3′ ends from reverse-transcribed cDNA in two separate steps. Uteri were removed from several outbred ICR mice 1 day after parturition, and total RNA was isolated. To clone the 3′ end of the cDNA, an adaptor-poly d(T) primer was used for RT from the mRNA. The resulting cDNA served as a template for PCR amplification of sequence between a primer specific for the adaptor sequence at the 3′ end and an MAT-specific primer as described in MATERIALS AND METHODS. The MAT-specific primer was derived from a sequence contained in the third exon of the mouse gene (MMEX3; Figure 1B), which was isolated by screening a mouse genomic library with the human MAT cDNA under low stringency conditions. RACE products were analyzed by gel electrophoresis and Southern blotting. A single clone (MMAT2) was found that hybridized to the MMEX3 probe and was a fragment of approximately the expected size (~700 bp; Figure 1A), based on the human cDNA. Sequences corresponding to most of exon 3 and all of exons 4, 5, and 6 were identified after the fragment was cloned into a pGEM vector, sequenced, and compared with the human cDNA and gene. The sequence was verified on both strands using two subclones (MMAT2a and MMAT2b) of MMAT2 (Figure 1A).

Sequence upstream of exon 4 was obtained using the 5′ RACE strategy as outlined in MATERIALS AND METHODS. This technique involves tailing the initial cDNA strand with dCTP, followed by PCR amplification with a gene-specific primer derived from MMAT2 sequence and an adaptor primer capable of annealing to the poly C tail. The 5′ RACE product (MMAT1; Figure 1A) was shown to contain sequence corresponding to exons 1, 2, and 3 by comparison to the human sequence. Together, MMAT1 and MMAT2 comprise a cDNA of 1072 bp, of which the coding sequence is 75% and 90% identical to human and rat MAT cDNA, respectively.

Using MMEX3 as a probe, a murine MAT genomic DNA clone was isolated from a library prepared from strain 129/Sv DNA. MMAT2, several derivative fragments of MMAT2, and a segment of the human cDNA corresponding to exons 1 and 2 were used to map subclones of the original λ clone. Organization of the exons within the genomic DNA is schematically represented in Figure 1B, along with the strategy used for sequencing. Like the human gene (Gaire *et al.*, 1994), six exons comprise the mouse gene and each exon is composed of the same number of nucleotides, with two exceptions (Table 1): exon 1 contains 157 bp, rather than 155, and exon 6 is shorter by 51 bp in the mouse (248 bp) in contrast to the human (299 bp; Gaire *et al.*, 1994). The size of each intron listed in Table 1 was estimated by restriction enzyme mapping and Southern blotting of the genomic subclones. Note that the exact size of exon 1 as reported here is based on the cDNA obtained by RT-PCR, and has not been confirmed by primer extension analysis of the mRNA. However, genomic sequence upstream of exon 1 shows that the center of the TATA box (i.e., at the second T) in the promoter is at position −20 relative to the proposed start site of transcription (our unpublished results), which falls within the consensus range (−36 to −20) determined by Bucher (1990). This observation suggests that MMAT1 most likely contains a full-length 5′-untranslated region.

The sequence of the exons derived from subclones of the original genomic segment is compared with the mouse cDNA sequence in Figure 1C. There appear to be seven nucleotide differences between the cDNA and genomic sequences, five of which are confined to the 5′- and 3′-untranslated regions in exons 1 and 6, respectively. In exon 4, there are two positions in which there is an A in the cDNA but a G in the gene. The first difference, at nucleotide 631, is in the wobble position in the codon for lysine, and does not affect the amino acid residue. In contrast, the nucleotide difference at position 651 results in substitution of an aspartic acid residue for a glycine residue encoded by the genomic sequence. Because this amino acid change is not conservative, and a glycine residue is encoded at this position in both the rat and human cDNAs, it is probable that the nucleotide difference at position 651 is due to an error in replication by TAQ polymerase in the 3′ RACE procedure. Although the other six differences may be due to replication errors as well, changes in

the noncoding regions also can be ascribed to differences in sequence between the mouse strains used for cloning the cDNA and the gene (ICR and 129/Sv, respectively).

Both the mouse and rat MAT cDNAs differ from the human sequence in several ways. First, the rodent sequences contain two in-frame ATG codons in exon 1 at bp positions 41 and 50 (34 and 43 in the rat), which are boxed in Figure 1C. Only the latter codon is found in the human cDNA. The context in which the first codon occurs in the rodent sequences is not as favorable as the second for translation initiation, according to the scanning-model guidelines outlined by Kozak (reviewed in Kozak, 1989). The downstream ATG codon contains a highly conserved purine residue at position −3, whereas the upstream codon contains a T at this position; a purine at −3 is usually indicative of a strong initiation codon (Kozak, 1989). Initiation from the upstream ATG would result in a protein product containing a three-amino acid extension at the amino-terminus of the pre domain, as depicted in Figure 2. Second, translation of MAT protein in both the mouse and the rat terminates early with respect to the human; the codon at position 839 (835 in the rat) is followed by two adjacent termination codons (Figure 1C), resulting in a protein which is three amino acids shorter than the human gene product (Figure 2). However, recombinant human MAT produced in Chinese hamster ovary cells and its corresponding activated form lack the three carboxy-terminal amino acids encoded by the human gene (Barnett *et al.*, 1994), suggesting that these residues do not contribute to the known biological activity of MAT. Lastly, the rodent cDNAs and the murine gene contain one polyadenylation consensus sequence (boxed in Figure 1C), in contrast to two sites that were recently reported for a human cDNA derived from mesangial cells (Marti *et al.*, 1992) and for the human gene (Gaire *et al.*, 1994).

As might be expected, the murine and rat deduced amino acid sequences are more homologous to each other (87%) than either sequence is to the human (70%). The consensus PRCGVPDV sequence in the prodomain containing the cysteine residue involved in enzyme latency is perfectly conserved among the three species (Figure 2). In addition, positioning of the histidine residues that coordinate the zinc atom in the sequence HEXGHXXGXXH is also maintained. The protein product from all three species, mouse, rat, and human, is predicted to contain a threonine residue that immediately precedes the HEXGHXXGXXH region and is not found in other MMPs (arrow, Figure 2; Birkedal-Hansen *et al.*, 1993).

Expression and Localization of MAT mRNA in Female Reproductive Organs

The rodent postpartum uterus undergoes rapid involution as the organ returns to pre-pregnancy size, a process that requires approximately 5 days (reviewed in Mullins and Rohrlich, 1983). MAT is expressed in the rat uterus immediately after parturition, but is undetectable by day 5 (Sellers and Woessner, 1980; Woessner and Taplin, 1988; Quantin *et al.*, 1989). As a matrix-degrading metalloproteinase, MAT may have an important role in remodeling of this tissue during involution. To determine whether MAT is expressed in the mouse postpartum uterus in a manner similar to the rat, a Northern analysis of total RNA at different time points was performed using radiolabeled MMAT2 cDNA as a probe. MAT transcripts of approximately 1.1 kb were abundant from 6 h to 1.5 days postpartum, with message levels decreasing at days 2.5 and 3.5 (Figure 3A). By day 4.5, little, if any, mRNA could be detected; the size of the uterus was also indistinguishable from that of nonpregnant animals at this time point. MAT expression does occur in the uterus of both virgin and pregnant animals, but at a lower level than that in the involuting uterus (Figure 3B). MAT mRNA was detectable in the uterus of 4- and 5-wk old females by RT-PCR, but not by Northern blotting (Table 2), suggesting that a high level of MAT expression correlates with the onset of the estrus cycle. The specific stage(s) of the cycle during which MAT is expressed is currently under investigation (Rudolph and Matrisian, unpublished data).

The difference in overall morphology between the uterus at 1.5 days versus 3.5 days postpartum is apparent in the bright-field photographs in panels A and B of Figure 4. The uterus becomes reduced in size primarily through loss of collagen (Harkness and Moralee, 1956), and a marked decrease in the surface area of the lumenal epithelium can be observed (Figure 4). MAT transcripts were localized in transverse sections of involuting uterus by in situ hybridization. As shown in Figure 4, panel C, hybridization of the antisense riboprobe was intense and continuous along the epithelium lining the lumen of the uterus at 1.5 days. A similar pattern of expression was observed in the rat using a rat MAT riboprobe (our unpublished results). High-power magnification (Figure 4, panel E) of the section clearly shows silver grains only in the epithelial cells. In addition, hybridization was observed in some glands of the uterus (see Figure 4, panel C). At 3.5 days postpartum (Figure 4, panels D and F), hybridization was greatly diminished. MAT localizes to the lumenal epithelium in uterus samples from adult virgin and pregnant animals as well (our unpublished results).

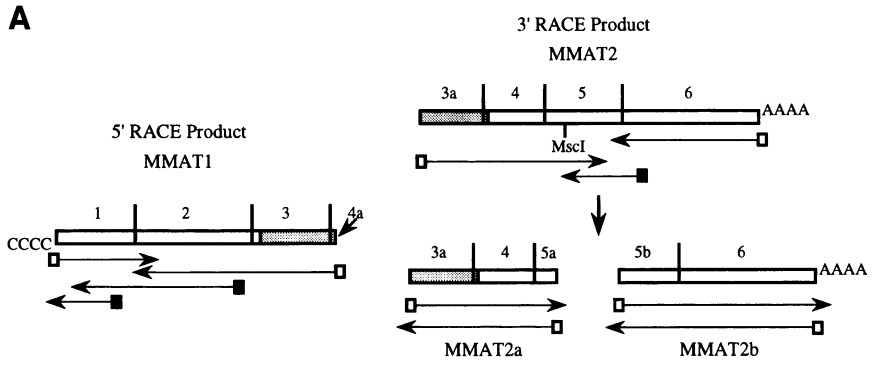

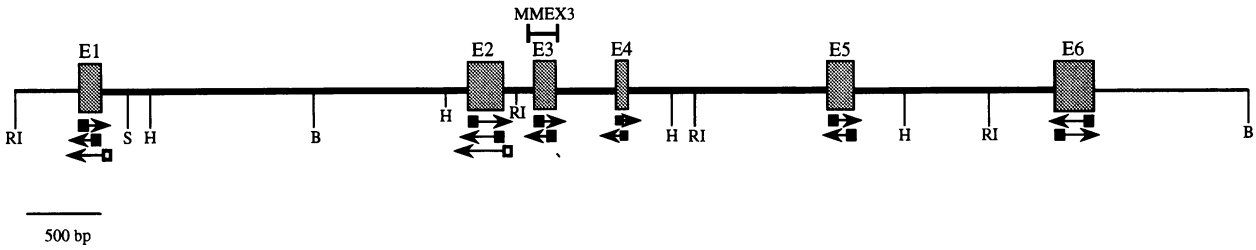

C

```
cDNA    1  CGGAAAACATCAAAGTAGCTCTGAGAACAATCGCCTGTTGATGGCAGCTATGCAGCTCACCCTGTTCTGCTTTGTGTGTC
GENE       A G

                                                                                  1 | 2
       81  TGCTGCCAGGCCACCTGGCCCTGCCACTGTCCCAGGAAGCTGGAGATGTGAGCGCACATCAGTGGGAACAGGCTCAGAAT

      161  TATCTTAGAAAATTTTACCCTCATGACTCTAAAACAAAGAAGGTCAATAGTCTAGTGGACAACCTCAAGGAAATGCAGAA

      241  GTTCTTTGGCCTGCCCATGACTGGAAAACTCTCCCCCTACATCATGGAAATAATGCAGAAACCTAGGTGTGGAGTGCCAG

                                                                        2 | 3
      321  ATGTTGCAGAATACTCACTAATGCCAAACAGTCCAAAATGGCATTCCAGAATTGTCACCTACAGAATTGTATCCTATACT

      401  TCAGACTTACCTCGGATCGTAGTGGATCAAATCGTGAAAAAAGCTCTCAGAATGTGGAGTATGCAGATCCCACTGAACTT

                                                                  3 | 4
      481  CAAGAGGGTTAGTTGGGGGACTGCGGATATCATAATTGGCTTCGCAAGGAGAGATCATGGAGACAGCTTCCCCTTTGATG

      561  GGCCAGGGAACACTCTAGGTCATGCCTTCGCACCTGGGCCAGGCCTAGGCGGAGATGCTCACTTTGACAAAGATGAGTAC
                                                                                  G
                                                              4 | 5
      641  TGGACTGATGATGAGGACGCAGGAGTGAACTTCCTGTTTGCTGCCACCCATGAATTTGGCCACTCTCTGGGTCTGAGTCA
                   G
                (ASP → GLY)
      721  CTCTTCTGTTCCCGGTACTGTGATGTACCCTACCTATCAAAGAGACTACTCAGAAGACTTCAGTCTTACAAAGGACGACA

                                                          5 | 6
      801  TTGCAGGCATTCAGAAGTTATATGGAAAGAGGAACACGCTGTGATAGATGCAGACAGATCACAGAAACGGTCTGCACTCA
                   .
      881  CTGGGTCCTCCATTGCATCCCTCAGCTGGCATGAACAAATGCCCTTCCTGAGCTGCACCTGTCTCCCTCTTCCTTGTGCT
                                                                C                 T
      961  GTGGATGGATTTTGCACATCCCTCTGAGGGTCATCTTGACGGAATGATTCTGACTAATCTCAGGTAACATGAAGTTGCGA
                G
     1041  GACATCAACAATAAATGTCATGTGCACAAATA
```

Figure 1.

Table 1. Exon-intron junctions in the mouse matrilysin gene

Exon/intron	Exon-intron junctions	Exon size (bp)	Intron size (bp)
1	....CTCAGgtatatcctt	157	~2300
2	tgtctaccagAATTA... ...TACAGgtgaggctca	227	~200
3	gtgccttcagAATTG... ...GAGAGgtaagaatgg	149	~450
4	ctgtttgcagATCAT... ...CGCAGgtacagtatc	129	~1350
5	ctgtctgtagGAGTG... ...ATATGgtaataatca	162	~1400
6	ttcttatcagGAAAG... ...AAATA.....	248	

Exons were mapped in the genomic subclones described in the MATERIALS AND METHODS. Mapping was performed by restriction enzyme digestion and Southern hybridization using the mouse and human cDNAs as probes. Exon and partial intron sequence was obtained using the primers indicated in Figure 1B for sequencing. Exon-intron boundaries were located by the GT/AG rule and comparison to the cDNA sequence. Intron sizes were estimated on agarose gels from the distance in base pairs between diagnostic restriction enzyme sites in the exons.

Because the mammary gland also undergoes major changes during juvenile development, pregnancy, lactation, and involution (reviewed in Neville and Daniel, 1987), we analyzed total RNA extracted from the left inguinal and thoracic mammary glands by RT-PCR for MAT expression at different stages in the reproductive cycle. Using primers derived from the exon 4/5 sequence and the 3′-untranslated region, the expected 292-bp product was detected from tissue at metestrus II and during lactation (6 h, 2.5 days, and 5.5 days postpartum) and involution (3 days post-weaning) (Table 2). However, the level of expression appears to be very low, because transcripts could not be localized by in situ hybridization or detected by Northern blotting (Table 2). The stages at which MAT is expressed in the uterus and mammary gland are summarized in Table 2.

Analysis of MAT Expression in Major Adult Tissues

Other major organs in the adult mouse were examined by Northern blotting of total RNA to determine whether MAT is expressed in normal tissue. As shown in Figure 5, a high level of expression, comparable to that in the postpartum uterus, was evident only in the small intestine. MAT transcripts were not usually detectable in other organs of the gastrointestinal tract (colon and stomach). RNA extracted from the male gonad, which includes the testis, epididymis, and extra-testicular ducts, showed variability in the profile of bands obtained among individual animals. For example, in sample A, a band at approximately 1.1 kb was present at low intensity; in sample B, at least two higher molecular weight bands hybridized weakly to the MMAT2 cDNA probe, but not the expected 1.1-kb band. It should be noted that several high molecular weight bands hybridize to the same probe in total RNA from the small intestine and involuting uterus (arrowheads, Figure 5). However, as shown in Figure 6, the expected 292-bp product was generated by RT-PCR of total RNA from the sample B gonad (compare with postpartum uterus and small intestine). Several organs that were negative for MAT expression by Northern analysis, namely the colon, kidney, liver, lung, skeletal muscle, skin, and stomach, also showed

Figure 1 cont. Sequence analysis of murine MAT cDNA and structure of the gene. (A) The exon boundaries in the 5′ and 3′ RACE products (MMAT1 and MMAT2, respectively) are denoted by the vertical bars. MMAT1 (546 bp) contains sequence corresponding to exons 1, 2, and 3, and 13 nucleotides of exon 4 (designated 4a). The poly C tail was added to the 3′ end of the noncoding strand as part of the PCR cloning strategy. MMAT2 (666 bp) contains sequence corresponding to all but 21 nucleotides of exon 3 (designated 3a), and exons 4, 5, and 6, as well as the poly A tail. Sequence overlap between MMAT1 and MMAT2 is indicated by the stippled boxes. The 3′ RACE product was cleaved at the *Msc*I restriction site in exon 5 and the resulting fragments (MMAT2a and MMAT2b) were subcloned for sequencing on both strands. The location of primers used for sequencing and the extent of sequence determined are shown by the arrows. A solid box on the arrow indicates a sequence-specific primer, and an open box indicates a universal primer (SP6, T7, or T3). (B) An 8.5-kb fragment from the genomic clone containing the exons (stippled boxes) in the gene is diagrammed. Primers derived from the 5′ and 3′ ends of each exon as indicated were used for dideoxy sequencing. Exon and partial intron sequence was obtained from genomic subclones as detailed in MATERIALS AND METHODS. The MMEX3 fragment, which was isolated from the C3H genomic library and contains all of exon 3 and 26 bp of flanking intron sequence, was used to derive the RACE primers and to probe the 129/Sv library. B = *Bam*HI, H = *Hin*dIII, RI = *Eco*RI, and S = *Sph*I. (C) The cDNA sequence from MMAT1 and MMAT2 is shown compared with exon sequence derived from the genomic clone. The two possible translation initiation codons are boxed, as well as the termination codons (TGATAG) and polyadenylation consensus sequence (AATAAA). The A at position 651 in the cDNA gives rise to an aspartic acid residue, whereas the G at this position in exon 4 of the gene encodes a glycine, as indicated. Nucleotides comprising the gene-specific primers used in the 5′ (←) and 3′ (→) RACE techniques are underlined. GenBank accession numbers: L36244 (cDNA), L36243 (genomic exon 1), L36242 (genomic exon 2), L36241 (genomic exon 3), L36240 (genomic exon 4), L36239 (genomic exon 5), L36238 (genomic exon 6).

```
mouse   (MAA)MQLTLFCFVCLLPGHLALPLSQEAGDVSAHQWEQAQNYLRKFYPHDSKTK
rat          R     RI      C          E T L             L
human   --- MR  VL A       S     P    GM EL      D  KR  LY  E

mouse   KVNSLVDNLKEMQKFFGLPMTGKLSPYIMEIMQKPRCGVPDVAEYSLMPNSPKW
rat      AT A  K R          E       RV                  F
human   NA   EAK            I  M NSRVI                    F

mouse   HSRIVTYRIVSYTSDLPRIVVDQIVKKALRMWSMQIPLNFKRVSWGTADIIIGF
rat        T          T    FL       R
human   T KV          R   H T  RL S   N  GKE   H RK V       M

mouse   ARRDHGDSFPFDGPGNTLGHAFAPGPGLGGDAHFDKDEYWTDGEDAGVNFLFAA
rat       G    N                                    S      V
human     GA    Y          A       T          E  R    SSL I   Y

mouse   THEFGHSLGLSHSSVPGTVMYPTYQRDYSEDFSLTKDDIAGIQKLYGKRNTL---
rat        L       G     SS       G H                      K ---
human      L       MG    D NA      GNGDPQN K SQ   K          SNSRKK
```

Figure 2. Comparison of the deduced amino acid sequences of mouse, rat, and human MAT. The predicted amino acid sequence of mouse MAT is shown compared with the rat and human sequences. Only the amino acid residues of rat and human MAT that differ from the murine sequence are depicted. In the mouse and rat, initiation of translation at the first ATG in Figure 1C would result in the three additional residues (MAA) shown in parentheses at the amino terminus. The putative boundaries of the pre and pro domains are indicated by the solid and open arrows, respectively. The conserved PRCGVPDV and HEXGHXXGXXH sequences are underlined, and the T residue unique to MAT is denoted by an arrow. The arrowhead marks the amino acid residue (G) in the mouse sequence, which is the same as that encoded by the rat and human cDNAs and murine gene, but differs from that encoded by the murine cDNA.

low levels of the 292-bp product (Figure 6). Southern blotting and hybridization with MMAT2 cDNA verified that this product originated from MAT mRNA (our unpublished results). Brain, heart, and spleen were consistently negative by both Northern and RT-PCR analysis.

We used in situ hybridization to localize MAT mRNA in organs that showed expression by Northern and RT-PCR analysis. In the small intestine, expression was detected in the duodenum, jejunum, and ileum (Figure 7, panels A–C). Transverse sections of each region revealed a pattern of hybridization that circumscribed the base of the tissue and was less intense in the duodenum (Figure 7, panel A) in contrast to the jejunum (Figure 7, panel B) and ileum (Figure 7, panel C). Sense-strand riboprobes did not hybridize to the sections, as shown for the ileum in Figure 7, panel D. Furthermore, expression was not detected in any region of the colon (Figure 7, panel E), although the mRNA could be detected by RT-PCR (Figure 6).

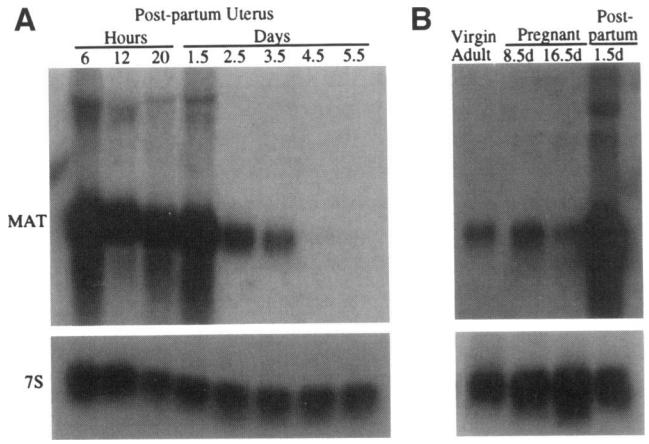

Figure 3. MAT expression in the uterus. Total cellular RNA was isolated from the uterus of one animal at each time point indicated. The MAT transcript at approximately 1.1 kb was detected by Northern blotting and hybridization with radiolabeled mouse MAT cDNA. The blot was stripped and re-probed for cytoplasmic 7S RNA as a control for equal loading. Each lane contains 10 μg of total RNA. RNA isolated from the uterus at different time points after parturition is shown in panel A, with day 0.5 defined as noon on the day when pups are first found. RNA from the uterus of adult virgin and pregnant animals is shown in comparison to the postpartum uterus in panel B.

Table 2. Expression of MAT in female reproductive organs

Mammary gland		Uterus	
Juvenile		Juvenile	
P28	$-^R$	P28	$-^N/+^R$
P35	$-^R$	P35	$-^N/+^R$
Virgin Adult		Virgin Adult	$+^N$
Estrus	$-^R$	Pregnant	
Metestrus I	$-^R$	8.5 d	$+^N$
Metestrus II	$-^N/+^R$	16.5 d	$+^N$
Diestrus	$-^R$	Involuting	
Proestrus	$-^R$	6 h	$+^N$
Lactating		12 h	$+^N$
6 h	$-^N/+^R$	20 h	$+^N$
2.5 d	$-^N/+^R$	1.5 d	$+^N$
6.5 d	$-^N/+^R$	2.5 d	$+^N$
Involuting	$-^N/+^R$	3.5 d	$+^N$
3 d	$-^N/+^R$	4.5 d	$-^N$

Expression of MAT was analyzed by Northern blotting (N) and/or RT-PCR (R) of total RNA extracted from the left thoracic and inguinal mammary glands and the uterus at the indicated stages. The forward and reverse primers for RT-PCR were derived from cDNA sequence spanning exons 4 and 5 and from the 3′-untranslated region in exon 6, respectively, giving rise to a product of 292 bp.

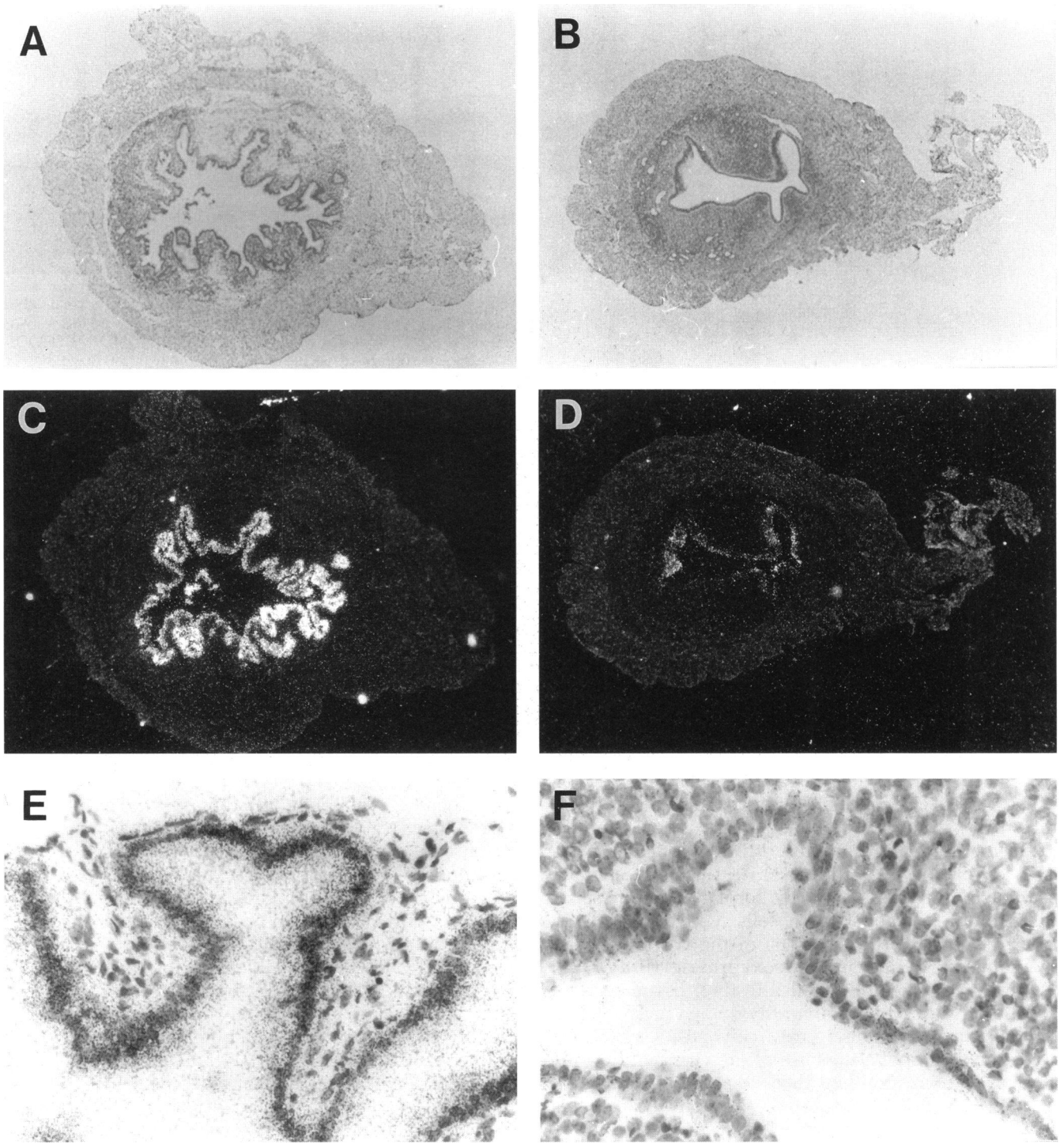

Figure 4. Localization of MAT mRNA in the postpartum uterus. Transverse sections of the uterus at days 1.5 (A, C, and E) and 3.5 (B, D, and F) postpartum were analyzed by in situ hybridization with the antisense MAT ribroprobe. Photographs were taken with either bright-field (A, B, E, and F) or dark-field (C and D) illumination at 12.5× (A–D) and 500× magnification (E and F).

High-power magnification of the jejunum in panel F of Figure 7 shows that MAT transcripts are confined to cells at the base of the crypts of Lieburkuhn, or the intestinal glands (arrows). The site of hybridization of the riboprobe was identical in the duodenum and ileum as well, although not every crypt in the duode-

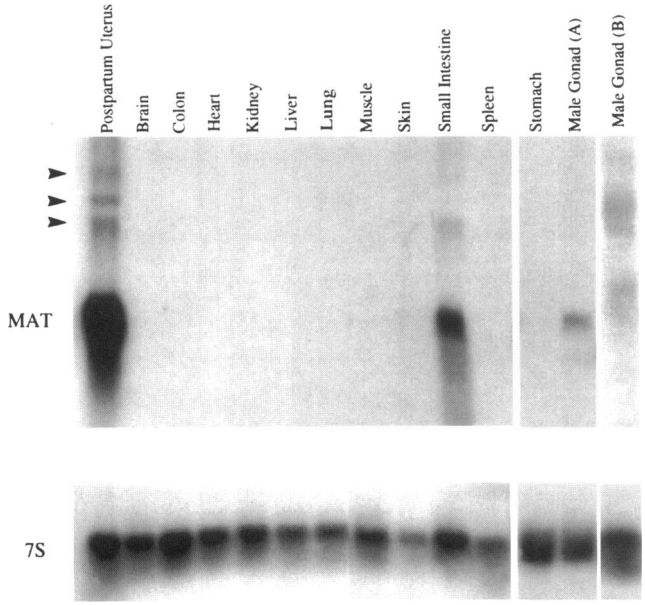

Figure 5. Expression of MAT in normal adult tissues. MAT expression in the tissues indicated was assessed by Northern analysis as in Figure 3. Each lane contains 15–20 μg of total RNA.

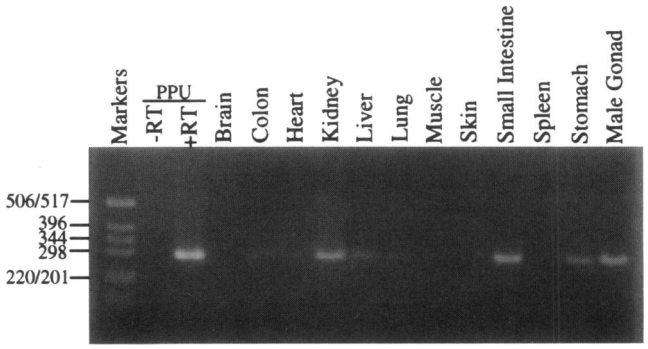

Figure 6. RT-PCR analysis of MAT expression in normal adult tissues. 0.5 μg of total RNA extracted from the indicated tissues was used for RT-PCR as described in MATERIALS AND METHODS. Twenty microliters of each 100-μl reaction was analyzed by gel electrophoresis (1.4% agarose) and ethidium bromide staining. A control reaction in which the RT step was omitted (−RT) is shown for postpartum uterus RNA and is representative of the results obtained for the other organ RNAs. Marker sizes (in bp) are indicated to the left.

num was positive (see Figure 7, panel A). Primitive columnar cells that give rise to the differentiated cells of the villi flank the base of the crypt, whereas the granular Paneth cells reside at the base proper. The positioning of the cells and the pattern of hybridization suggested that MAT is expressed in the Paneth cells. To verify this interpretation, a riboprobe derived from a cDNA encoding a Paneth-cell marker, cryptdin-1, was used for in situ hybridization of the small intestine. As shown in panel G of Figure 7 for the jejunum, the pattern of hybridization clearly overlapped that of MAT (arrows). In a complementary approach, we used an assay for DNA synthesis to distinguish between Paneth cells, which do not mitose, and other primitive cells in the crypt. Animals were injected with bromodeoxyuridine (BrdU) 1 h before harvesting the small intestine; tissue sections were then stained with an antibody against BrdU. As depicted in panel H of Figure 7, cells positive for BrdU uptake reside above the base of the crypt and do not appear to correspond to those that hybridize to the MAT cRNA. Taken together, these results indicate that the Paneth cells are the source of MAT expression in the small intestine.

Northern and RT-PCR analysis revealed that MAT is expressed in the adult male gonad. Therefore, in situ hybridization was used to localize the mRNA in parasagittal sections of the gonad from males at 6 wk, 10 wk, and 10 mo of age. An example of the hybridization pattern in tissue from a 10-wk old animal is shown in Figure 8. The MMAT2 antisense riboprobe hybridized intensely to epithelial cells lining the efferent ducts, which transport sperm from the testis to the epididymis (Figure 8, panel A). A group of efferent ducts entering the initial segment of the epididymis was positive for MAT expression (Figure 8, panels C and D). In addition, a low level of hybridization was observed in the proximal area of the initial segment of the epididymis (Figure 8, panel D), as well as in at least part of the cauda, where mature, fully differentiated sperm accumulate in the lumen (Figure 8, panels E and F). However, this pattern seemed to be restricted to animals older than 6 wk of age (our unpublished results). In both areas of the epididymis, the pattern of hybridization was not as uniformly intense in every cell as in the efferent ducts. The testis, caput and corpus epididymis, and vas deferens were negative at all ages of adult that were examined.

Although MAT mRNA was identified in the adult colon, kidney, liver, lung, skeletal muscle, skin, and stomach by RT-PCR, we were unable to localize expression by in situ hybridization. However, MAT transcripts were identified fortuitously in an extrahepatic branch of the bile duct by in situ hybridization of neonatal liver sections (P1 stage). As shown in Figure 9, the MMAT2 antisense riboprobe hybridized specifically to epithelial cells lining the duct (Figure 9, panel A), whereas the sense-strand riboprobe did not (Figure 9, panel B). Hybridization of the cRNA to ducts within the liver at P1 and adult stages could not be detected. Presumably, MAT transcripts detected in the adult by RT-PCR would also localize to similar extra-hepatic structures; these were not present in the tissue samples that were analyzed by in situ hybridization. Also, in other organs, the level of expression may be too low to detect by methods that lack the

sensitivity of RT-PCR, or only a few cells may be producing the message. Other organs containing glandular-like epithelium were examined by in situ hybridization as well; the prostate, bladder, pancreas, salivary gland, and esophagus were all negative.

Expression of MAT during Embryonic and Postnatal Development

Both embryonic and perinatal development of the mouse are accompanied by extensive tissue remodeling and turnover of ECM molecules, which may involve MMPs and their inhibitors (reviewed in Matrisian and Hogan, 1990). For example, Brenner *et al.* (1989) have shown that transcripts for collagenase, stromelysin-1, and TIMP-1 increase at the blastocyst stage and during differentiation of embryonal carcinoma cells into endoderm. Furthermore, the mRNA for the 72- and 92-kDa gelatinases, TIMP-1 and TIMP-3, has been localized to specific embryonic tissues by in situ hybridization (Nomura *et al.*, 1989; Reponen *et al.*, 1992, 1994; Apte *et al.*, 1994). To determine whether MAT is also expressed during embryogenesis, a combination of RT-PCR and in situ hybridization was used to analyze embryos from E9.5 to E18 (day E0.5 defined as noon on the day after coitus). Sagittal sections of paraffin-embedded embryos at E9.5, E14, E15, E16, and E18 were probed with MMAT2 cRNA. Specific hybridization of the antisense riboprobe was not detected at any of these stages, except in epithelial cells lining the residual lumen of the maternal uterus (our unpublished results). The deciduum was also negative for MAT expression. However, we were able to detect very low levels of the 292-bp PCR product from total RNA at stages E9.5, as well as E15.5, E16.5, and E17.5 (arrow, Figure 10). Intermediate stages were negative by ethidium bromide staining (e.g., see E13.5, Figure 10). It is possible that the PCR product obtained at stage E9.5 could, in part, be due to the presence of maternal MAT transcripts in the uterus, because it is more difficult to dissect embryos away from uterine tissue at this stage. The 292-bp band was detected when the PCR products were blotted and probed with radiolabeled MMAT2 cDNA (our unpublished results).

We examined several organs that showed MAT expression in the adult at different stages in postnatal development to establish a time course of the appearance of MAT mRNA. Expression at P1 and P7 was assessed primarily by in situ hybridization, whereas a combination of methods (Northern blotting, RT-PCR, and in situ hybridization) was used to analyze expression at P13, P17, P32, and P42. As shown in Table 3, MAT transcripts were first detectable by RT-PCR in the colon and stomach at 2–2.5 wk (P13 and P17) in juvenile development. Expression in the small intestine and liver was evident as early as the P1 stage by RT-PCR and in situ hybridization, respectively. It is possible that expression in the other organs occurs at P1 and P7, but at a level or in areas that were not detectable by in situ hybridization. MAT mRNA was discernible in the juvenile small intestine and male gonad by Northern analysis, albeit at low levels, at stage P13 (Table 3). However, in both organs, MAT transcripts could not be detected by in situ hybridization at this stage, in contrast to the adult. Furthermore, MAT mRNA in the immature uterus was detectable only by RT-PCR (Table 2). Taken together, these findings show that although expression of MAT occurs in the juvenile small intestine, male gonad, and uterus, significant levels of message are associated with the onset of maturity.

DISCUSSION

We have cloned the mouse homologue of the MMP MAT and have analyzed its expression pattern in the developing embryo and in neonatal and adult animals. Overlapping cDNAs (MMAT1 and MMAT2) were obtained from the involuting postpartum uterus using the 5′ and 3′ RACE techniques, and the predicted protein sequence was shown to be 70% and 87% identical to the human and rat MAT sequences, respectively. Mapping of a genomic clone demonstrated that the structure of the gene is similar to that of the human in that six exons encode the pre, pro, and catalytic domains that comprise MAT. Several motifs related to enzyme activity, including the PRCGVPDV and HEXGHXXXGH sequences, are well conserved in the mouse cDNA. Most notably, in the mouse and rat cDNAs, translation terminates three codons upstream of the analogous human sequence, which should result in a slightly shorter mature protein (170 residues versus 173 in the human protein). Interestingly, recombinant human MAT also lacks these residues, presumably due to proteolytic processing (Barnett *et al.*, 1994). Finally, in exon 1 of both rodent sequences, there are two ATG codons separated by nine nucleotides, with the second codon corresponding to the ATG in the human sequence. Based on the Kozak guidelines, translation most likely initiates at this second ATG in the mouse sequence, although this has not been demonstrated experimentally.

Expression and localization of MAT mRNA in normal adult tissues was assessed by a combination of Northern analysis, RT-PCR, and in situ hybridization. MAT was found to be expressed at significant levels (i.e., detectable by Northern blotting) in the epithelial cells lining the lumen and some glands of the cycling, pregnant, and involuting uterus, in the Paneth cells in small intestinal crypts, and in epithelial cells lining the efferent ducts of the male reproductive tract. In situ analysis revealed hybridization in part of the initial segment and cauda of the epididymis in mature adult

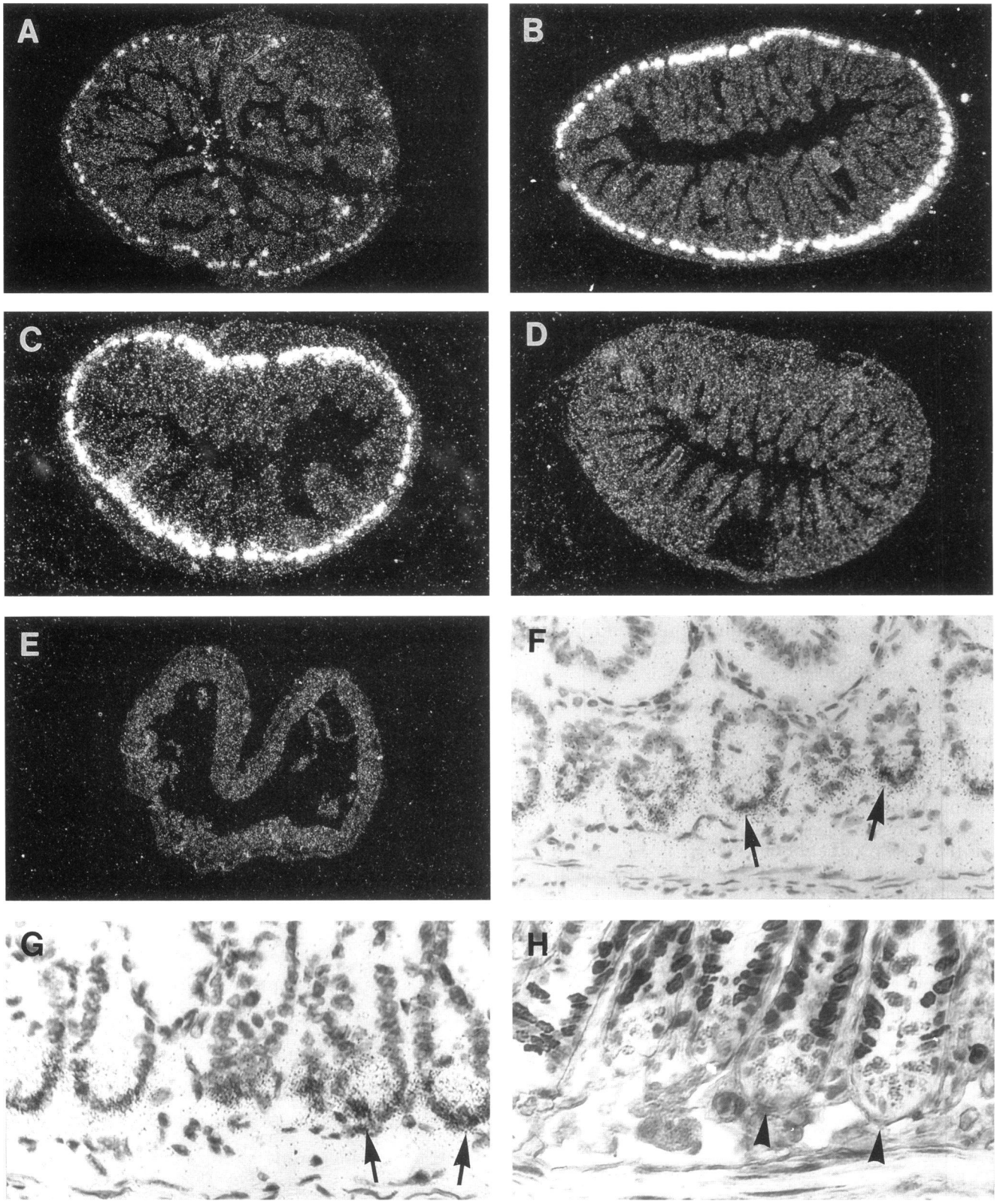

Figure 7.

males. Expression in the adult colon, kidney, liver, lung, skeletal muscle, skin, stomach, and in nonpregnant, lactating, and involuting mammary gland was detectable only by RT-PCR. Although MAT mRNA could be localized to a branch of the bile duct exiting the liver, at least at the P1 stage of juvenile development, by in situ hybridization, the site(s) of expression in organs other than the small intestine, uterus, and male gonad could not be identified using this technique. It is possible that the level of MAT expression in these tissues is below the threshold of sensitivity of the in situ assay, if only a few cells are synthesizing MAT mRNA, and at very low levels. Furthermore, areas of tissue where MAT is expressed may not have been represented in the sections analyzed by in situ hybridization. In some of these tissues, the source of MAT expression may be transient infiltrating cells, rather than resident parenchymal cells. For example, it is known that MAT is expressed in both unstimulated peripheral blood monocytes from humans and in monocyte-derived macrophages allowed to differentiate in vitro, although expression is not detectable in alveolar macrophages (Busiek *et al.*, 1992). However, hybridization of the MAT antisense riboprobe to mononuclear phagocytes was not observed in any of the mouse tissue sections examined.

In situ hybridization with the MAT riboprobe localized MAT mRNA to glandular-like epithelium (i.e., simple columnar epithelial cells) in the organs in which the gene is expressed in the mouse. Restriction of MAT expression primarily to epithelial cells parallels the pattern of expression observed in both normal and neoplastic tissue from humans. For example, MAT mRNA has been detected in a number of adenomas and adenocarcinomas from various tissues (Basset *et al.*, 1990; McDonnell *et al.*, 1991; Muller *et al.*, 1991; Pajouh *et al.*, 1991; Newell *et al.*, 1994). In addition, matrilysin protein is produced in a rectal carcinoma-derived cell line (Miyazaki *et al.*, 1990), in cutaneous squamous-cell carcinomas at the tumor-stroma interface (Karelina *et al.*, 1994), and in the basal layer of fetal epidermis, the outer root sheath of adult hair follicles, and in the secretory cells of the eccrine glands (Karelina *et al.*, 1994); both the mRNA and protein are found in the glandular epithelium of the cycling endometrium (Rodgers *et al.*, 1993). Expression of MAT in epithelial cells is unusual, in that most of the MMPs are produced in stromal cells (reviewed in Crawford and Matrisian, 1995). The finding that MAT expression is essentially restricted to epithelial cells, as well as the fact that MAT is not expressed by all glandular epithelium in the mouse, suggest that the elaboration of MAT by these cells in specific organs is important in processes of tissue function. Although we cannot rule out the possibility that the mRNA synthesized in these organs is not translated into protein, in previous studies on human tissue, we and others have found a good correlation between expression of the message and the protein for MAT (McDonnell *et al.*, 1991; Powell *et al.*, 1993; Rodgers *et al.*, 1993).

Because the ECM is extensively re-organized during both embryonic and postnatal development, expression of MAT was examined at different time points in the ontogeny of the mouse using the same techniques described for the adult. Transcripts were detected by RT-PCR of total RNA from embryos at 9.5, 15.5, 16.5, and 17.5 days postcoitum. Despite these results, we were unable to localize MAT mRNA in sections of embryos at any stage in development. To date, only the gelatinases and TIMP-1 and -3 have been localized to specific tissues during embryogenesis (Nomura *et al.*, 1989; Reponen *et al.*, 1992, 1994; Apte *et al.*, 1994). With the exception of the salivary gland, expression of the 72-kDa gelatinase occurs primarily in mesenchymal tissue from stage E10 to E15 (Reponen *et al.*, 1992). The 92-kDa gelatinase shows a highly restricted expression pattern, in that the mRNA is only detected in cells of the osteoclast lineage (Reponen *et al.*, 1994). Similarly, high levels of TIMP-1 are expressed in osteogenic tissues in the head and limb at later stages in development (Nomura *et al.*, 1989). TIMP-3 expression, on the other hand, occurs not only in cartilage, but also in the skin, liver, and in epithelium of bronchial tubes, the bile duct, colon, and kidney (Apte *et al.*, 1994), all of which are potential areas of MAT expression, at least in the adult. Because it is likely that MAT is expressed in the epithelial cells of embryonic organs at stages where it was detected by RT-PCR, these findings raise the possibility that TIMP-3 and MAT are coordinately regulated in some tissues. We are currently investigating the use of more sensitive techniques, such as in situ RT-PCR, to attempt to localize MAT transcripts during embryogenesis.

Organs that showed the presence of MAT transcripts by Northern blotting of adult RNAs were examined at different stages in juvenile development to determine the time course and qualitative level of expression. In the small intestine, expression was de-

Figure 7 cont. Localization of MAT mRNA to Paneth cells in the small intestine. Transverse sections of the duodenum (A), jejunum (B and F), ileum (C and D), and descending colon (E) were analyzed by in situ hybridization using the antisense MAT riboprobe (A–C, E, and F) or the sense-strand control (D). Photographs in panels A–E were taken with dark-field illumination at 30× magnification. High-power magnification (500×) of the jejunum (F) shows silver grains over the Paneth cells at the base of the intestinal crypts (arrows). An antisense cryptdin-1 riboprobe hybridizes to cells in the same location (arrows) in the jejunum (G; magnification = 640×). The sense-strand control was negative. In H, the arrowheads indicate cells lacking incorporation of BrdU in jejunum dissected from an animal injected with the nucleotide analogue. Magnification = 640×.

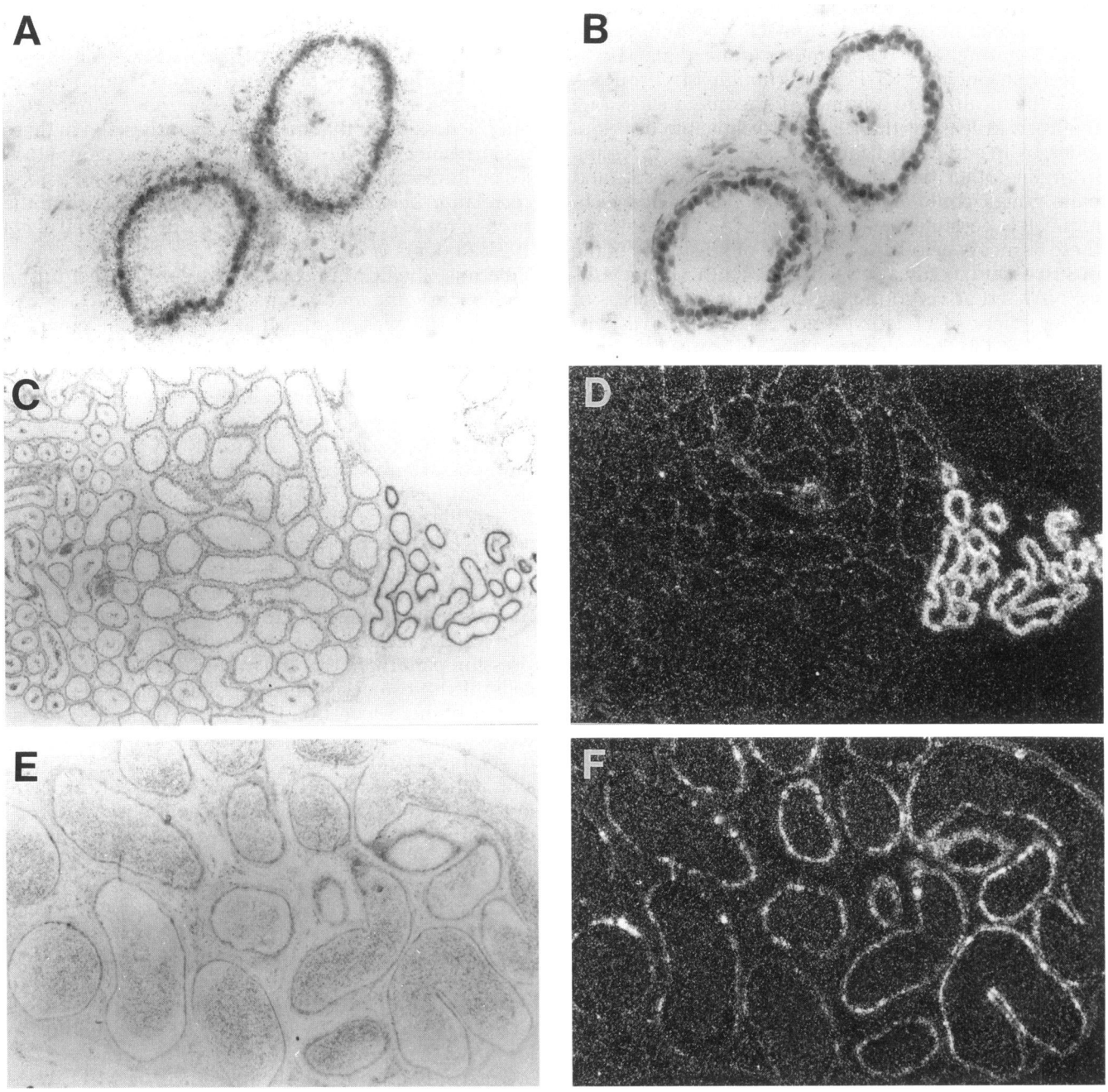

Figure 8. Localization of MAT mRNA in the male reproductive tract. Testis, epididymis, and extra-testicular ducts were dissected as a unit from a 10-wk old C57BL/6N male, fixed, embedded, sectioned parasagittally, and processed for in situ hybridization as described in MATERIALS AND METHODS. Shown in panels A and B are cross-sections of efferent ducts hybridized with either the antisense MAT riboprobe (A) or the sense-strand control (B). Magnification = 400×. Panels C (bright field) and D (dark field) show a low-power magnification (50×) of the efferent ducts (at right) entering the initial segment of the epididymis (at left). The section was hybridized with the antisense MAT riboprobe. A portion of the cauda is shown in panels E (bright field) and F (dark field) hybridizing to the same probe. Magnification = 40×. The sense-strand controls did not show hybridization above background.

tectable as early as the P1 stage by RT-PCR. However, the mRNA could not be localized by in situ hybridization, even at 2 wk of age. In contrast, transcripts for the enteric defensin cryptdin-1, which co-localize with MAT mRNA, could be detected in the majority of small intestinal crypts at P13, in agreement with results obtained by others (Ouellette *et al.*, 1989; Bry *et al.*, 1994). Although crypts have formed by 2 wk into

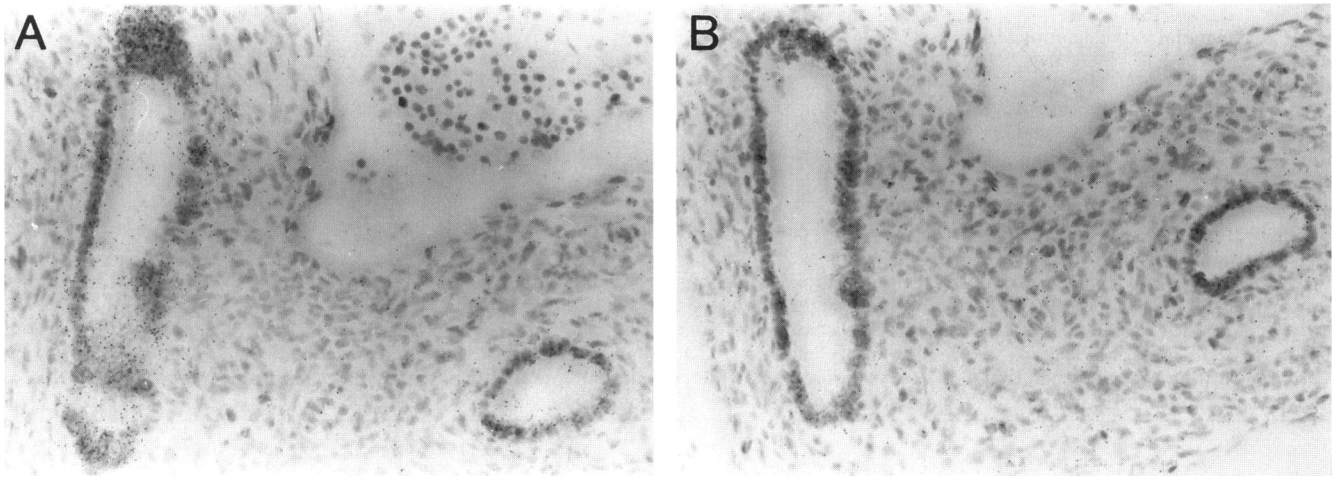

Figure 9. Localization of MAT mRNA in the neonatal liver. Cross-sectional segments of the torso from a P1 animal were embedded in paraffin wax and transverse sections were made and analyzed by in situ hybridization. Panels A and B show high-power magnification (400×) of a section containing the liver. The antisense MAT riboprobe hybridized to a branch of the bile duct exiting the liver (A), whereas the sense-strand control did not (B).

postnatal development, the small intestine continues to undergo morphogenetic changes until P21 (Bry *et al.*, 1994). MAT expression in the male gonad was faintly discernible by Northern analysis at the P13 stage, but not by in situ hybridization, indicating that the message is produced at low levels in the sexually immature animal. In fact, expression in the cauda was not observed in animals at 6 wk of age. Likewise, MAT mRNA in the juvenile uterus could be amplified by RT-PCR at P28 and P35, but was not detectable by Northern blotting except in cycling females. As in the adult, expression in the colon, liver, and stomach of juvenile animals could be detected only by RT-PCR. Taken together, these results show that MAT expression occurs at relatively low levels in the juvenile small intestine, uterus, and male gonad, and increases with maturation of the mice into adulthood. Expression in other organs, such as the colon and liver, appears to be consistently low in both juveniles and adults. Based on these data, we propose that MAT expression in the mouse is more closely linked with differentiated organ function than with morphogenetic processes occurring in developing and immature tissue. It is possible that low levels of MAT expression, i.e., detectable only by RT-PCR, are important in certain organs in highly localized areas; however, it seems likely that the intense levels of expression of this MMP must correlate with as yet unknown functional processes in the adult organs examined. This idea lends a new perspective to the role of matrix-degrading enzymes in vivo. Although numerous studies have shown a strong correlation between the elaboration of MMPs and degradative and invasive events during tumor progression, an enzyme such as MAT may have additional roles. For example, we have demonstrated that the overexpression of MAT in a non-metastatic colon carcinoma cell line results in increased tumorigenicity, suggesting that MAT may be involved in cell growth and proliferation (Witty *et al.*, 1994).

Although the pattern of MAT mRNA expression does not explain its specific function(s), it does provide clues as to possible roles for this MMP. We have shown that MAT mRNA appears in the uterus exclusively in resident epithelial cells, and, in agreement with previous work (Woessner and Taplin, 1988), at particularly high levels during involution. The process of involution involves the degradation of collagen, elastin, proteoglycans, and muscle proteins (reviewed in Mullins and Rohrlich, 1983). MAT is able to degrade fibronectin, proteoglycans, and elastin (Quantin *et al.*, 1989; Murphy *et al.*, 1991). Furthermore, it can digest

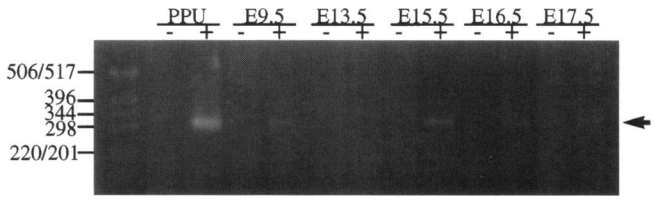

Figure 10. RT-PCR analysis of MAT transcripts in embryonic RNAs. 0.25 μg of total RNA isolated from whole embryos at different times postcoitum (with day 0.5 defined as noon on the day the seminal plug was found) was subjected to RT-PCR analysis. PCR product in 75 μl of the 100-μl reaction was concentrated by ethanol precipitation and electrophoresed in a 1.4% agarose gel as shown in Figure 6. From postpartum uterus RNA, an amount of product equivalent to 37.5 μl of the original reaction volume was also included as a positive control. Products obtained in the absence (−) and presence (+) of reverse transcriptase activity are shown for each time point.

Table 3. Postnatal expression of MAT

Organ	P1	P7	P13	P17	P32	P42	>P56
Colon	$-^{I}$	$-^{I}$	$-^{N}/+^{R}$	$-^{N}/+^{R}$	$-^{N}/+^{R}$	$-^{N}/+^{R}$	$-^{N}/+^{R}$
Liver	$+^{I}$	X	$-^{N}/+^{R}$	$-^{N}/+^{R}$	$-^{N}/+^{R}$	$-^{N}/+^{R}$	$-^{N}/+^{R}$
Male gonad	$-^{I}$	$-^{I}$	$-^{I}/+^{N}$	$+^{N}$	$+^{N}$	$+^{N}$	$+^{N}$
SI	$-^{I}/+^{R}$	$-^{I}/+^{R}$	$-^{I}/+^{N}$	$+^{N}$	$+^{N}$	$+^{N}$	$+^{N}$
Stomach	$-^{I}$	$-^{I}$	$-^{N}/+^{R}$	$-^{N}/+^{R}$	$-^{N}/+^{R}$	$-^{N}/+^{R}$	$-^{N}/+^{R}$

Pups at stages P1 and P7 were sacrificed by decapitation and segments of torso were fixed in paraformaldehyde and embedded in paraffin wax. Expression of MAT mRNA in organs at these stages was assessed by in situ hybridization (I) of tissue cross-sections using the MMAT2 riboprobe. In addition, small intestine (SI) was dissected from P1 and P7 animals for RNA extraction and RT-PCR (R) analysis as described in MATERIALS AND METHODS. Expression in organs dissected from animals from P13 to adulthood (≥P56) was examined initially by Northern blotting (N), and then by RT-PCR if negative by Northern analysis. Note that the P13 small intestine and male gonad were also analyzed by in situ hybridization. The X denotes stages that were not examined.

collagen strands initially cleaved by collagenase (Quantin *et al.*, 1989), of which the smooth muscle cells of the myometrium appear to be the major source (Blair *et al.*, 1986). Because expression of degradative enzymes in the uterus differs spatially and temporally, as well as in cell-type and substrate specificity (Rudolph and Matrisian, unpublished data), MAT may cooperate with other MMPs and proteases to effect complete tissue resorption in the uterus. Because MAT can activate procollagenase and progelatinase A (Quantin *et al.*, 1989; Crabbe *et al.*, 1994), an equally attractive possibility is that MAT expression is required for the activity of these MMPs in the involuting uterus. Changes in the architecture of uterine tissue also occur during the estrus cycle and pregnancy, when MAT is expressed, and may involve similar mechanisms. Furthermore, MAT may have a related role in matrix remodeling in the lactating and involuting mammary gland as well, although the level of expression is much lower than that in the uterus. Expression of MAT at specific stages in the estrus cycle may be subject to regulation by steroid hormones, as has been suggested for this MMP and others in the human endometrium (Osteen *et al.*, 1994; Rodgers *et al.*, 1994) and in the male rat, where castration results in the induction of MAT mRNA in epithelial cells of the ventral prostate as it undergoes involution (Powell, W.C., Domann, F.E., Mitichen, J.M., Matrisian, L.M., Nagle, R.B., and Bowden, G.T., Matrilysin expression in the involuting rat ventral prostate, Powell, Domann, Mitichen, Matrisian, Nagle, and Bowden, unpublished data).

Like the involuting uterus, the small intestine is characterized by rapid tissue and cell turnover. MAT mRNA was detected in the crypts in all three regions of the small intestine and was localized to the Paneth cells that reside at the extreme base of the crypts. Because Paneth cells express defense molecules including lysozyme (Speece, 1964), TNF (Keshav *et al.*, 1990; Tan *et al.*, 1993), CD1 Ag (Lacasse and Martin, 1992), and bacteriocidal peptides called cryptdins (enteric defensins), they are believed to have a role in controlling intestinal microorganisms (Eisenhauer *et al.*, 1992; Selsted *et al.*, 1992). Unlike villus cells, which have a rapid turnover rate (3–4 days) and are shed into the lumen of the small intestine, Paneth cells degenerate every 3 wk and are phagocytized by adjacent columar cells (Cheng, 1974; Bjerknes and Cheng, 1981). MAT may have some role in this degenerative process, perhaps by mediating degradation of the basement membrane. Alternatively, MAT may affect the differentiation or maturation of Paneth cells by modulating the composition of the local ECM; alterations in the ECM have been shown to change the functional and morphological phenotype of some cells (reviewed in Lin and Bissell, 1993). Another possibility is that MAT expression may affect processing of other molecules produced by Paneth cells. It was recently demonstrated that a recombinant, truncated version of TNF-α can be cleaved in vitro to its mature form by MAT, among other MMPs (Gearing *et al.*, 1994). The mRNA for this cytokine is produced in Paneth cells, although the protein product has not been detected yet in either murine or human small intestine (Keshav *et al.*, 1990; Tan *et al.*, 1993). Similarly, cryptdins are synthesized as larger precursors in these cells and are processed to their biologically active 6-kDa forms by an unknown mechanism, leading to the supposition that MAT may be involved in the activation of procryptdins.

We speculate that MAT may have some role in sperm maturation in the male reproductive tract, perhaps by a mechanism that may also involve proteolytic processing. High levels of MAT mRNA are synthesized in the epithelial cells of the efferent ducts, which originate from the testis as three to seven individual tubules that unite to form the single duct of the epididymis (reviewed in Fekete, 1941). We observed intense expression of MAT along the entire length of the efferent ducts, and, in mature animals, in the epididymis in the proximal area of the initial segment and part of the cauda. Although it is not known

whether the rete testis expresses MAT, the testis proper, the caput and corpus epididymis, and the vas deferens, which exits the cauda, were all shown to be negative by in situ hybridization. The nature of the transcripts produced in the male gonad are of particular interest; several high molecular weight bands were visible on Northern blots of some samples, either in addition to or in lieu of the expected 1.1-kb band. This pattern was especially characteristic of adult animals, and also occurred in RNA from the small intestine and involuting uterus. These high molecular weight bands may represent unprocessed transcripts, or may be a result of cross-hybridization of the MMAT2 cDNA probe to as yet undescribed MAT-related messages. Regardless, identification of mRNA encoding a matrix-degrading enzyme in epithelial cells of the male reproductive tract is intriguing, particularly in light of its differential localization in the extra-testicular duct system. Precursor regions in both the α and β subunits of PH-30, a sperm surface protein that has been implicated in sperm-egg fusion, contain metalloproteinase domains that align with those found in snake venom proteins (Wolfsberg *et al.*, 1993); furthermore, the pro-α subunit contains the consensus active-site HEXGHXXXGH motif. This metalloproteinase domain has been proposed to function in early spermatogenesis, perhaps by processing of the β subunit (Wolfsberg *et al.*, 1993). The α subunit is cleaved to its mature form in the testis, whereas the β subunit is not completely processed until sperm have reached the cauda (Blobel *et al.*, 1990). In rodents, caudal sperm are fully fertilization competent, a state that is believed to be mediated by biochemical modifications of surface proteins such as PH-30, PH-20, and AH-50 as the sperm transit through the extra-testicular duct system (Phelps *et al.*, 1990). Taken together, these observations raise the possibility that MAT may have such a role in processing of sperm antigens during maturation, either directly or indirectly, given its localization to the efferent ducts and portions of the epididymis. Another possibility is that MAT expression may affect the expression or function of other molecules differentially localized along the extra-testicular duct system, such as sulfated glycoproteins 1 and 2 (reviewed in Hermo *et al.*, 1994). Defining the role of MAT in this system and other organs can be addressed by genetically manipulating MAT levels in vivo. Experiments are underway to generate MAT-deficient mice by gene targeting and to examine the effect of the mutation on normal processes, with particular focus on gastrointestinal and reproductive function.

ACKNOWLEDGMENTS

The authors thank Drs. Howard Crawford, Mireille Gaire, and William Powell for a critical and thorough evaluation of the manuscript; Zenaida Magbanua and Parul Patel for help in sequencing; Bart Lutterbach, Kaylon Bruner, and Anna Park for their initial work in screening the genomic libraries; Dr. Michael Jones for the gift of embryonic RNAs; Cathy Chayko and Drs. Loren Hoffman and Marie-Claire Orgebin-Crist for help in identifying histological structures; Dr. Andre Ouellette for the gift of cryptdin-1 cDNA and many enlightening discussions; and Jane Wright for photography assistance. This work was supported by the National Institutes of Health (grant RO1-CA60867 to L.M.M.), the American Cancer Society (postdoctoral fellowship to C.W.), and National Institutes of Health training grants (T32-CA09592 to K.H. and C.W., and T32-HD07043 to L.R.).

REFERENCES

Alexander, C.M., and Werb, Z. (1989). Proteinases and extracellular matrix remodeling. Curr. Opin. Cell Biol. *1*, 974–982.

Apte, S.S., Hayashi, K., Seldin, M.F., Mattei, M.-G., Hayashi, M., and Olsen, B.R. (1994). Gene encoding a novel murine tissue inhibitor of metalloproteinases (TIMP), TIMP-3, is expressed in developing mouse epithelia, cartilage, and muscle, and is located on mouse chromosome 10. Dev. Dynamics *200*, 177–197.

Balmain, A., Krumlauf, R., Vass, J.K., and Birnie, G.D. (1982). Cloning and characterization of the abundant cytoplasmic 7S RNA from mouse cells. Nucleic Acids Res. *10*, 4259–4279.

Barnett, J., Straub, K., Nguyen, B., Chow, J., Suttman, R., Thompson, K., Tsing, S., Benton, P., Schatzman, R., Chen, M., and Chan, H. (1994). Production and characterization of human matrilysin (PUMP) from recombinant Chinese hamster ovary cells. Protein Expression Purification *5*, 27–36.

Basset, P., Bellocq, J.P., Wolf, C., Stoll, I., Hutin, P., Limacher, J.M., Podhajcer, O.L., Chenard, M.P., Rio, M.C., and Chambon, P. (1990). A novel metalloproteinase gene specifically expressed in stromal cells of breast carcinomas. Nature *348*, 699–704.

Birkedal-Hansen, H., Moore, W.G.I., Bodden, M.K., Windsor, L.J., Birkedal-Hansen, B., DeCarlo, A., and Engler, J.A. (1993). Matrix metalloproteinases: a review. Crit. Rev. Oral Biol. Med. *4*, 197–250.

Bjerknes, M., and Cheng, H. (1981). The stem-cell zone of the small intestinal epithelium: evidence from Paneth cells in the adult mouse. Am. J. Anat. *160*, 51–63.

Blair, H.C., Teitelbaum, S.L., Ehlich, L.S., and Jeffrey, J.J. (1986). Collagenase production by smooth muscle: correlation of immunoreactive with functional enzyme in the myometrium. J. Cell. Physiol. *129*, 111–123.

Blobel, C.P., Myles, D.G., Primakoff, P., and White, J.M. (1990). Proteolytic processing of a protein involved in sperm-egg fusion correlates with acquisition of fertilization competence. J. Cell Biol. *111*, 69–78.

Brenner, C.A., Adler, R.R., Rappolee, D.A., Pedersen, R.A., and Werb, Z. (1989). Genes for extracellular matrix-degrading metalloproteinases and their inhibitor, TIMP, are expressed early during mammalian development. Genes Dev. *3*, 848–859.

Bry, L., Falk, P., Huttner, K., Ouellette, A., Midtvedt, T., and Gordon, J. (1994). Paneth cell differentiation in the developing intestine of normal and transgenic mice. Proc. Natl. Acad. Sci. USA *91*, 10335–10339.

Bucher, P. (1990). Weight matrix descriptions of four eukaryotic RNA polymerase II promoter elements derived from 502 unrelated promoter sequences. J. Mol. Biol. *212*, 563–578.

Busiek, D.F., Ross, F.P., McDonnell, S., Murphy, G., Matrisian, L.M., and Welgus, H.G. (1992). The matrix metalloproteinase matrilysin (PUMP) is expressed in developing human mononuclear phagocytes. J Biol. Chem. *267*, 9087–9092.

Cheng, H. (1974). Origin, differentiation and renewal of the four main epithelial cell types in the mouse small intestine. Am. J. Anat. *141*, 521–536.

Chomczynski, P., and Sacchi, N. (1987). Single-step method of RNA isolation by acid guanidinium thiocyanate-phenol-chloroform extraction. Anal. Biochem. *162*, 156–159.

Crabbe, T., Smith, B., O'Connell, J., and Docherty, A. (1994). Human progelatinase A can be activated by matrilysin. FEBS Lett. *345*, 14–16.

Crawford, H.C., and Matrisian, L.M. (1995). Tumor and stromal expression of matrix metalloproteinases and their role in tumor progression. Invasion Metastasis (*in press*).

Eisenhauer, P.B., Harwig, S.S.S.L., and Lehrer, R.I. (1992). Cryptdins: antimicrobial defensins of the murine small intestine. Infect. Immun. *60*, 3556–3565.

Fekete, E. (1941). Histology. In: Biology of the Laboratory Mouse, ed. G. Snell, New York: Dover Publications, 133–137.

Frohman, M.A., Dush, M.K., and Martin, G.R. (1988). Rapid production of full-length cDNAs from rare transcripts: amplification using a single gene-specific oligonucleotide primer. Proc. Natl. Acad. Sci. USA *85*, 8998–9002.

Gaire, M., Magbanua, Z., McDonnell, S., McNeil, L., Lovett, D.H., and Matrisian, L.M. (1994). Structure and expression of the human gene for the matrix metalloproteinase matrilysin. J. Biol. Chem. *269*, 2032–2040.

Gearing, A.J.H., Beckett, P., Christodoulou, M., Churchill, M., Clements, J., Davidson, A.H., Drummond, A.H., Galloway, W.A., Gilbert, R., Gordon, J.L., Leber, T.M., Mangan, M., Miller, K., Nayee, P., Owen, K., Patel, S., Thomas, W., Wells, G., Wood, L.M., and Woolley, K. (1994). Processing of tumour necrosis factor-α precursor by metalloproteinases. Nature *370*, 555–557.

Harkness, R.D., and Moralee, B.E. (1956). The time course and route of loss of collagen from the rat's uterus during post-partum involution. J. Physiol. *132*, 502–508.

Hermo, L., Oko, R., and Morales, C.R. (1994). Secretion and endocytosis in the male reproductive tract: a role in sperm maturation. Int. Rev. Cytol. *154*, 106–189.

Hirose, T., Patterson, C., Pourmotabbed, T., Mainardi, C.L., and Hasty, K.A. (1993). Structure-function relationship of human neutrophil collagenase: identification of regions responsible for substrate specificity and general proteinase activity. Proc. Natl. Acad. Sci. USA *90*, 2569–2573.

Karelina, T.V., Goldberg, G.I., and Eisen, A.Z. (1994). Matrilysin (PUMP) correlates with dermal invasion during appendageal development and cutaneous neoplasia. J. Invest. Dermatol. *103*, 482–487.

Keshav, S., Lawson, L., Chung, L.P., Stein, M., Perry, V.H., and Gordon, S. (1990). Tumor necrosis factor mRNA localized to Paneth cells of normal murine intestinal epithelium by in situ hybridization. J. Exp. Med. *171*, 327–332.

Kozak, M. (1989). The scanning model for translation: an update. J. Cell Biol. *108*, 229–241.

Lacasse, J., and Martin, L.H. (1992). Detection of CD1 mRNA in Paneth cells of the mouse intestine by in situ hybridization. J. Histochem. Cytochem. *40*, 1527–1534.

Lin, C.Q., and Bissell, M.J. (1993). Multi-faceted regulation of cell differentiation by extracellular matrix. FASEB J. *7*, 737–743.

Marti, H.-P., McNeil, L., Thomas, G., Davies, M., and Lovett, D.H. (1992). Molecular characterization of a low-molecular-mass matrix metalloproteinase secreted by glomerular mesangial cells as PUMP-1. Biochem. J. *285*, 899–905.

Matrisian, L.M. (1990). Metalloproteinases and their inhibitors in matrix remodeling. Trends Genet. *6*, 121–125.

Matrisian, L.M. (1992). The matrix-degrading metalloproteinases. BioEssays *14*, 455–463.

Matrisian, L.M., and Hogan, B.L.M. (1990). Growth factor-regulated proteases and extracellular matrix remodeling during mammalian development. Curr. Top. Dev. Biol. *24*, 219–259.

McDonnell, S., Navre, M., Coffey, R.J., and Matrisian, L.M. (1991). Expression and localization of the matrix metalloproteinase pump-1 (MMP-7) in human gastric and colon carcinomas. Mol. Carcinog. *4*, 527–533.

Miyazaki, K., Hattori, Y., Umenishi, F., Yasumitsu, H., and Umeda, M. (1990). Purification and characterization of extracellular matrix-degrading metalloproteinase, matrin (Pump-1), secreted from human rectal carcinoma cell line. Cancer Res. *50*, 7758–7764.

Muller, D., Breathnach, R., Engelmann, A., Millon, R., Bronner, G., Flesch, H., Dumont, P., Eber, M., and Abecassis, J. (1991). Expression of collagenase-related metalloproteinase genes in human lung or head and neck tumours. Int. J. Cancer *48*, 550–556.

Muller, D., Quantin, B., Gesnel, M.C., Millon-Collard, R., Abecassis, J., and Breathnach, R. (1988). The collagenase gene family in humans consists of at least four members. Biochem. J. *253*, 187–192.

Mullins, D.E., and Rohrlich, S.T. (1983). The role of proteinases in cellular invasion. Biochim. Biophys. Acta *695*, 177–214.

Murphy, G., Allan, J.A., Willerbroch, F., Cockett, M.I., O'Connell, J.P., and Docherty, A.J.P. (1992). The role of the C-terminal domain in collagenase and stromelysin specificity. J. Biol. Chem. *267*, 9612–9618.

Murphy, G., Cockett, M.I., Ward, R.V., and Docherty, A.J.P. (1991). Matrix metalloproteinase degradation of elastin, type IV collagen, and proteoglycan: a quantitative comparison of the activities of 95 kDa and 72 kDa gelatinases, stromelysins-1 and -2 and punctuated metalloproteinase (PUMP). Biochem. J. *277*, 277–279.

Neville, M.C., and Daniel, C.W. (1987). The Mammary Gland: Development, Regulation, and Function, New York: Plenum Press.

Newell, K., Witty, J., Rodgers, W.H., and Matrisian, L.M. (1994). Expression and localization of matrix-degrading metalloproteinases during colorectal tumorigenesis. Mol. Carcinog. *10*, 199–206.

Nomura, S., Hogan, B.L.M., Wills, A.J., Heath, J.K., and Edwards, D.R. (1989). Developmental expression of tissue inhibitor of metalloproteinase (TIMP) RNA. Development *105*, 575–583.

Osteen, K.G., Rodgers, W.H., Gaire, M., Hargrove, R.T., Gorstein, F., and Matrisian, L.M. (1994). Stromal-epithelial interaction mediates steroidal regulation of metalloproteinase expression in human endometrium. Proc. Natl. Acad. Sci. USA *91*, 10129–10133.

Ouellette, A.J., Greco, R.M., James, M., Frederick, D., Naftilan, J., and Fallon, J.T. (1989). Developmental regulation of cryptdin, a corticostatin/defensin precursor mRNA in mouse small intestinal crypt epithelium. J. Cell Biol. *108*, 1687–1695.

Pajouh, M.S., Nagle, R.B., Breathnach, R., Finch, J.S., Brawer, M.K., and Bowden, G.T. (1991). Expression of metalloproteinase genes in human prostate cancer. J. Cancer Res. Clin. Oncol. *117*, 144–150.

Phelps, B.M., Koppel, D.E., Primakoff, P., and Myles, D.G. (1990). Evidence that proteolysis of the surface is an initial step in the mechanism of formation of sperm cell surface domains. J. Cell Biol. *111*, 1839–1847.

Popesko, P., Rajtova, V., and Horak, J. (1992). A Colour Atlas of Anatomy of Small Laboratory Animals, London, UK: Wolfe Publishing.

Powell, W.C., Knox, J.D., Navre, M., Grogan, T.M., Kittelson, J., Nagle, R.B., and Bowden, G.T. (1993). Expression of the metallopro-

teinase matrilysin in DU-145 cells increases their invasive potential in severe combined immunodeficient mice. Cancer Res. *53*, 417–422.

Quantin, B., Murphy, G., and Breathnach, R. (1989). Pump-1 cDNA codes for a protein with characteristics similar to those of classical collagenase family members. Biochem. J. *28*, 5327–5333.

Reponen, P., Sahlberg, C., Huhtala, P., Hurskainen, T., Thesleff, I., and Tryggvason, K. (1992). Molecular cloning of murine 72-kDa type IV collagenase and its expression during mouse development. J. Biol. Chem. *267*, 7856–7862.

Reponen, P., Sahlberg, C., Munaut, C., Thesleff, I., and Tryggvason, K. (1994). High expression of 92-kD type IV collagenase (gelatinase B) in the osteoclast lineage during mouse development. J. Cell Biol. *124*, 1091–1102.

Rodgers, W.H., Matrisian, L.M., Giudice, L.C., Dsupin, B., Cannon, P., Svitek, C., Gorstein, F., and Osteen, K.G. (1994). Patterns of matrix metalloproteinase expression in cycling endometrium imply differential functions and regulation by steroid hormones. J. Clin. Invest. *94*, 946–953.

Rodgers, W.H., Osteen, K.G., Matrisian, L.M., Navre, M., Giudice, L.C., and Gorstein, F. (1993). Expression and localization of matrilysin, a matrix metalloproteinase, in human endometrium during the reproductive cycle. Am. J. Obstet. Gynecol. *168*, 253–260.

Rugh, R. (1968). The Mouse: Its Reproduction and Development, Minneapolis, MN: Burgess Publishing.

Sellers, A., and Woessner, J.F., Jr. (1980). The extraction of a neutral metalloproteinase from the involuting rat uterus, and its action on cartilage proteoglycan. Biochem. J. *189*, 521–531.

Selsted, M.E., Miller, S.I., Henschen, A.H., and Ouellette, A.J. (1992). Enteric defensins: antibiotic peptide components of intestinal host defense. J. Cell Biol. *118*, 929–936.

Sires, U.I., Griffin, G.L., Broekelmann, T.J., Mecham, R.P., Murphy, G., Chung, A.E., Welgus, H.G., and Senior, R.M. (1993). Degradation of entactin by matrix metalloproteinases: susceptibility to matrilysin and identification of cleavage sites. J. Biol. Chem. *268*, 2069–2074.

Speece, A.J. (1964). Histochemical distribution of lysozyme activity in organs of normal mice and radiation chimeras. J. Histochem. Cytochem. *12*, 384–391.

Tan, X., Hsueh, W., and Gonzalez Crussi, F. (1993). Cellular localization of tumor necrosis factor (TNF)-alpha transcripts in normal bowel and in necrotizing enterocolitis: TNF gene expression by Paneth cells, intestinal eosinophils, and macrophages. Am. J. Pathol. *142*, 1858–1865.

Ward, J.M., Hagiwara, A., Anderson, L.M., Lindsey, K., and Diwan, B.A. (1988). The chronic hepatic or renal toxicity of di(2-ethylhexyl)phthalate, acetaminophen, sodium barbital, and phenobarbital in male B6C3F1 mice: autoradiographic, immunohistochemical, and biochemical evidence for levels of DNA synthesis not associated with carcinogenesis or tumor promotion. Toxicol. Appl. Pharmacol. *96*, 494–506.

Witty, J.P., McDonnell, S., Newell, K., Cannon, P., Navre, M., Tressler, R., and Matrisian, L.M. (1994). Modulation of matrilysin levels in colon carcinoma cell lines affects tumorigenicity in vivo. Cancer Res. *54*, 4805–4812.

Woessner, J.F., Jr. (1991). Matrix metalloproteinases and their inhibitors in connective tissue remodeling. FASEB J. *5*, 2145–2154.

Woessner, J.F., Jr., and Taplin, C. (1988). Purification and properties of a small latent matrix metalloproteinase of the rat uterus. J. Biol. Chem. *263*, 16918–16925.

Wolfsberg, T.G., Bazan, J.F., Blobel, C.P., Myles, D.G., Primakoff, P., and White, J.M. (1993). The precursor region of a protein active in sperm-egg fusion contains a metalloprotease and a disintegrin domain: structural, functional, and evolutionary implications. Proc. Natl. Acad. Sci. USA *90*, 10783–10787.